12 June 1998

ELSEVIER

Chemical Physics Letters 289 (1998) 341–349

CHEMICAL PHYSICS LETTERS

X-ray spectroscopic and quantum–chemical study of carbon tubes produced in arc-discharge

Alexander V. Okotrub [a,*], Lyubov G. Bulusheva [a], David Tomanek [b]

[a] *Institute of Inorganic Chemistry SB RAS, av. Lavrent'eva 3, Novosibirsk 630090, Russia*
[b] *Department of Physics and Astronomy, Michigan State University, East Lansing, MI 48824-1116, USA*

Received 29 January 1998; in final form 19 March 1998

Abstract

High-resolution CKα spectra have been obtained for samples containing carbon cage particles, synthesized using the arc-discharge graphite evaporation technique. The X-ray fluorescence spectrum of particles from the inner part of the cathode deposit was found to differ from that of the soot collected on the chamber walls. The dependence of the spectral profile on the geometry was investigated using quantum–chemical calculations of carbon nanotube fragments with different helical pitches. The spectrum of multiwall particles agrees best with the theoretical spectra of zig-zag tubes. The agreement between the spectra of tubular particles in the soot and the theoretical results is best for single-wall armchair tube structures. These studies are complemented by calculations of the frontier orbitals of nanotube fragments.

1. Introduction

Operating a graphite arc-discharge evaporation chamber at high temperatures in a helium atmosphere at reduced pressure makes it possible to synthesize carbon cage molecules — the fullerenes [1]. Under such conditions, carbon cage particles of various morphologies have been produced [2]. The carbon deposit formed on the cathode consists of multiwall structures: nanotubes, onions, capsules and, to some degree, glassy carbon [3–5]. Carbon soot formed on the cooled walls of the chamber contains single-wall tube-like particles [6,7].

In spite of substantial differences in the synthesis conditions, single-wall as well as multiwall particles consist of graphitic carbon. Electron microscopy investigations of nanotubes extracted from the deposit have shown that these systems contain carbon hexagons arranged in a helical fashion about the tube axis [4]. The helical pitch varies from tube to tube, with the chiral angle of the individual tubes ranging from 4 to 12° [5,8]. These tubes are most closely related to the zig-zag configuration designated as $(n,0)$ [9]. The determination of the atomic arrangement in the tubes is experimentally difficult and has been so far successful only for bundled nanotubes forming ropes [10]. These ropes consist, to a large degree, of (m,m) armchair-like tubes [10–12]. In these tubes, two of the hexagon sides are oriented along the perimeter. Theoretical studies have shown that the local arrangement of carbon atoms has a profound effect on the electronic structure of nanotubes [13–15]. In particular, it has been shown that

* Corresponding author. E-mail: TOMANEK@pa.msu.edu

0009-2614/98/$19.00
PII: S0009-2614(98)00405-9

tubes can be conducting or semiconducting depending on the chiral angle and the number of carbon hexagons along the tube perimeter [16,17].

One of the prominent experimental techniques to investigate electronic structure is X-ray fluorescence spectroscopy. CKα spectra contain the information about the electronic structure of carbon nanoparticles as a superposition of the local C2p electronic densities of states of the constituent atoms [18,19]. High-resolution X-ray spectra characterize the composition and chemical bonding in a given system [20,21].

In this Letter we present high-resolution CKα spectra of two samples produced using the arc-discharge graphite evaporation technique, one containing predominantly single-wall and the other multiwall structures. The significant difference between these spectra suggests that the electronic structure of carbon atoms in single- and multiwall systems is different. We use quantum–chemical calculations of carbon tube fragments with various chiralities to interpret the experimental results. In the theoretical part of this work, we focused on single-wall tubes. The interaction between carbon atoms in neighboring shells of multiwall structures is considerably weaker than the neighbor interaction within each graphitic layer. We assume that the inter-layer interaction cannot substantially change the profile of the X-ray spectrum. This is confirmed by the good agreement between the X-ray emission spectrum of graphite and the calculated spectrum of a two-dimensional graphite layer [22]. Previously published ab initio studies indicate that the structure of the occupied electronic states in single-wall and multiwall carbon nanotubes is very similar [23].

2. Experiment

The arc-discharge apparatus is described in Ref. [22]. The operated regime at 30 V and 30 kW is capable of evaporating approximately 200 g of graphite per hour. The cathode deposit is typically 40 mm high and 30 mm in diameter. Sample 1 is taken from the inner part of the deposit. It contains $\sim 20\%$ nanotubes, the rest consisting of carbon cones, onions and glassy carbon particles (Fig. 1.1). Sample 2 is obtained using the procedure outlined in Ref. [23] from the soot formed on the cold walls of the reaction chamber. It consists entirely of single-wall carbon nanotubes (Fig. 1.2.a,b).

CKα fluorescence spectra of samples 1 and 2 were recorded on the X-ray spectrometer 'Stearat'. The samples were mounted on a copper substrate and cooled down to liquid nitrogen temperature in the evacuated chamber of the X-ray spectrometer. The X-ray tube with a copper anode was operated at $U = 6$ kV and $I = 0.5$ A. The spectral resolution was ~ 0.5 eV. We used the NAP single crystal as a crystal-analyzer. The peculiarities of the use of this crystal to record CKα spectra have been described in Ref. [24]. This X-ray technique allowed us to determine the transition energy with an accuracy of ~ 0.3 eV.

The comparison between the CKα spectra of samples 1, 2 and a polycrystal graphite sample with a grain size of more than 10 μm is presented in Fig. 2. The general features of all these spectra are similar. We find that the vast majority of carbon atoms in samples 1 and 2 are of sp^2-type, which means that the nanoparticles predominately consist of hexagons. Four main features, marked as A′, A, B and C, can be distinguished in the spectra. The spectra were normalized to the value of the most intensive peak C. The relative intensities of the marked features are different. The peaks A and B in the CKα spectrum of sample 2 are more intensive, whereas the peak A′ is less intensive than the corresponding peaks in the spectrum of sample 1. We suppose that the main reason for these differences is the different morphology of the structures in the two samples. In order to verify this assumption, we studied the effect of the hexagon arrangement in the tube fragments on the

Fig. 1. Transmission electron micrographs of carbon cage-like nanoparticles with multiple walls, produced using the arc-discharge evaporation of graphite. (1) Sample 1, taken from the inner part of the cathode deposit. (2) Sample 2, obtained from the soot forming at the cold walls of the reaction chamber, in its raw form (a) and after processing according to Ref. [23] (b).

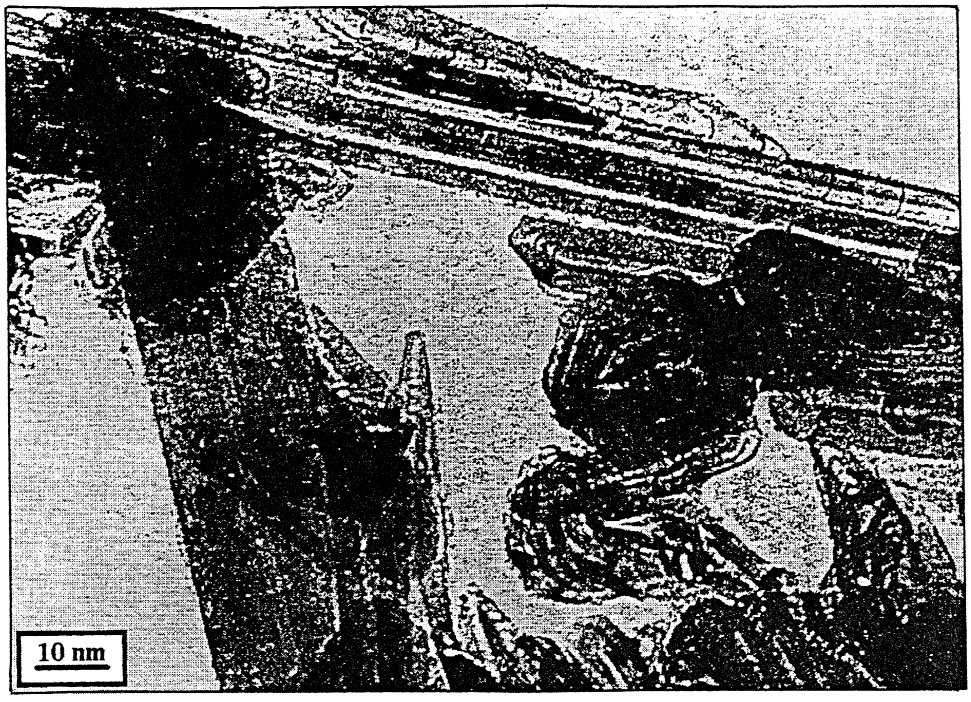

1

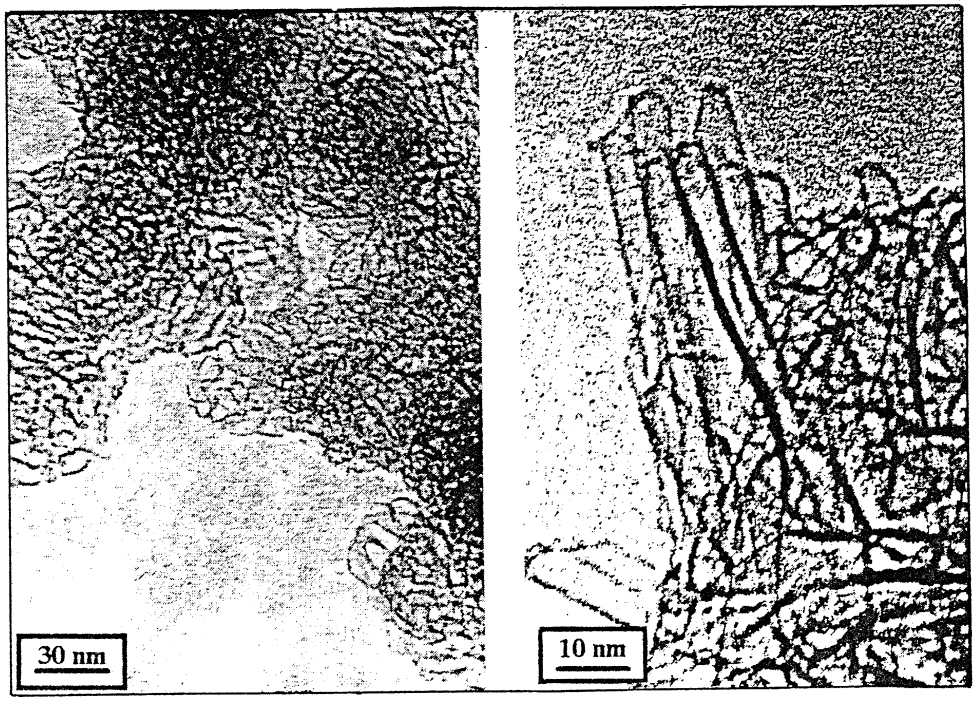

2

a b

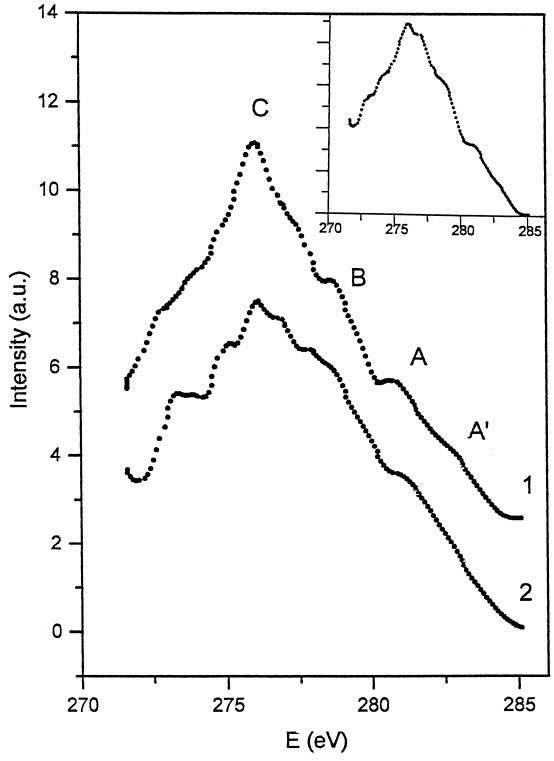

Fig. 2. CKα emission spectra of samples 1 and 2, micrographs of which are given in Fig. 1. The X-ray spectrum of nontextured graphite is shown in the inset for the sake of comparison.

structure of the occupied electronic states using quantum–chemical methods.

3. Calculation

We performed quantum–chemical calculations of carbon nanotube using the PM3 Hamiltonian [25] and the program GAMESS [26]. We considered our self-consistent field (SCF) calculations to be converged when the maximum change between subsequent iterations was below 10^{-8} for relative total energy differences and 10^{-5} for relative charge density differences. Here we present calculations for fragments of (10,0)–(5,5) nanotubes containing five hexagons in the axial direction. These tube fragments are shown in a perspective end-on view in Fig. 3. The dangling bonds at the ends of the nanotube fragments were saturated by hydrogen atoms. The carbon–carbon bonds have been assumed to be 1.42 Å long. The second-neighbor distance between carbon atoms along the tube perimeter has been taken as 2.43 Å. We used 1.1 Å for the carbon–hydrogen bond length. All atoms have been assumed to have the same radial distance from the tube axis, defining the tube radius. This definition of the cluster geometry ensures minimal distortion of the non-planar hexagons in the tubes spanning the whole range between armchair and zig-zag structures. The calculated diameters and chiral angles for the tubes we considered are summarized in Table 1.

4. Results and discussion

The tube fragments we consider contain equal numbers of carbon and hydrogen atoms. This allows us to estimate the relative stability of the tube fragments based on the calculated total energies (Table 1). We found the fragments of (10,0), (8,2) and (5,5) tubes to be thermodynamically more stable than the others. The features distinguishing these structures in the considered series of tubes are the achirality of (10,0) and (5,5) tubes and, from a theoretical viewpoint [27], the metallic conductivity of the infinite (8,2) tube. These results seem to support the com-

Table 1
Results of PM3 calculations for (n,m) nanotube fragments with different diameters and chiralities, but the same number of carbon atoms

Tube		(10,0)	(9,1)	(8,2)	(7,3)	(6,4)	(5,5)
diameter	(Å)	7.88	7.55	7.27	7.06	6.93	6.88
chiral angle	(°)	0.	6.46	12.75	18.75	24.35	30.
total energy	(E_h)	−532.94	−532.93	−532.94	−532.91	−532.77	−533.03
HOMO energy	(eV)	−5.4	−5.9	−5.6	−5.9	−6.5	−6.8
LUMO energy	(eV)	−4.3	−3.9	−1.6	−4.2	−3.7	−3.4
HOMO–LUMO gap	(eV)	1.1	2.0	4.0	1.7	2.8	3.4

monly shared view that, provided the same number of atoms, achiral tubes or chiral (l,k) tubes of 'metallic' character (i.e. $(l-k)$ is an integer multiple of three) are energetically preferred within the $(n,0)$–(m,m), $n = 2m$, series. The higher stability of the (5,5) tube fragment suggests that in thermal equilibrium and at low temperatures, the (m,m) armchair tubes should be more abundant.

The growth mechanism of nanotubes has not yet been well established, but growth by subsequent addition of hexagons at the open edge appears most likely. The point group symmetry of the $(n,0)$ nanotube fragments is affected by their length, expressed in the number N of carbon hexagons along the tube axis. Nanotube fragments with an odd N belong to the D_{nh} group, whereas nanotube fragments with an even N belong to the D_{nd} group. As we have shown in Ref. [28], the reactivity of $(n,0)$ nanotube fragments depends sensitively on the symmetry that is co-determined by their length. Nanotube fragments of D_{nd} symmetry are only thermodynamically stable when they carry an excess charge of $-2e$ or $+2e$. Consequently, growth of $(n,0)$ zig-zag nanotubes, which involves successive alternation between D_{nh} and D_{nd} fragments, is expected to proceed fastest in the presence of a net excess charge. Since such a charge can be provided most efficiently by the cathode of the carbon arc apparatus, it is not surprising to find that zig-zag nanotubes form abundantly under these conditions. The relative abundance of chiral nanotubes is possibly linked to the kinetics of formation, since the fastest growth is expected near the 'kinks' at the growing edge.

The reactivity of a cluster depends qualitatively on the size of the gap between the HOMO (highest occupied) and the LUMO (lowest unoccupied molecular orbital) [29]. Our results, presented in Table 1, indicate that fragments of metallic tubes are less reactive. Fragments of the armchair (m,m) tubes are described by the D_{mh} or D_{md} symmetry groups. The symmetry group is D_{md} if the cylindrical tube fragment contains an equal number N of hexagons along the tube axis for each stripe of hexagons. When the number N is different for adjoining stripes, the symmetry group is D_{mh}. We found the values of the HOMO–LUMO gap of 3.3 eV in the D_{5d} tube fragment and of 3.4 eV in the D_{5h} fragment to be similar. Consequently, we expect the reactivity of the (m,m) nanotube fragments not to depend on their length or symmetry and hence expect to observe the different fragments with equal probability. This indicates that the presence of external effects, such as a strong electric field, is not required for the formation of (m,m) tubes. Their accelerated formation, however, has been postulated to result from the catalytic action of metal atoms (Co or Ni) that reduce the activation barrier for the open-end growth [30].

A convenient tool to interpret the X-ray spectrum of a system in terms of its electronic structure is based on the MO LCAO (molecular orbitals represented as linear combinations of atomic orbitals) method and Koopman's theorem [31]. In this approximation, the X-ray spectral profiles are interpreted as the partial C2p electronic density of states in the ground state. The electronic spectrum of a finite cluster or a molecule is, of course, discrete. The location of a spectral line on the energy scale is given by the eigenvalue of the MO. The intensity of a given spectral line in the X-ray spectrum is obtained using the projection on the appropriate AOs in the ground state. It is calculated by summing up the squared coefficients of the 2p(C) AOs participating in the construction of a particular MO. The lines were normalized and convoluted with a Lorentzian curve with a full width at half maximum of 0.6 eV. The theoretical spectrum of a tube fragment was obtained by superposing the broadened molecular orbitals.

The calculated electronic spectra of 40 central atoms in fragments of various (n,m) nanotubes are shown in Fig. 3(II). These 40 central atoms form the 10 hexagons of the central part of cluster and are equally positioned at the cluster edges. We expect the electronic structure in the central region of the finite fragments to resemble closely the electronic structure of long, defect-free tubes. The calculated spectral profiles agree quite well with the experimental spectra, justifying a posteriori the use of quantum–chemical methods to interpret the X-ray spectra and to study the electronic structure of tubular carbon nanoparticles. Weak differences are observed in the theoretical spectra of the (10,0)–(5,5) tube series. Our results in Fig. 3(II) indicate a tendency for the intensity of peak B to increase with respect to the main peak C when changing from the zig-zag (10,0) tube to the armchair (5,5) tube.

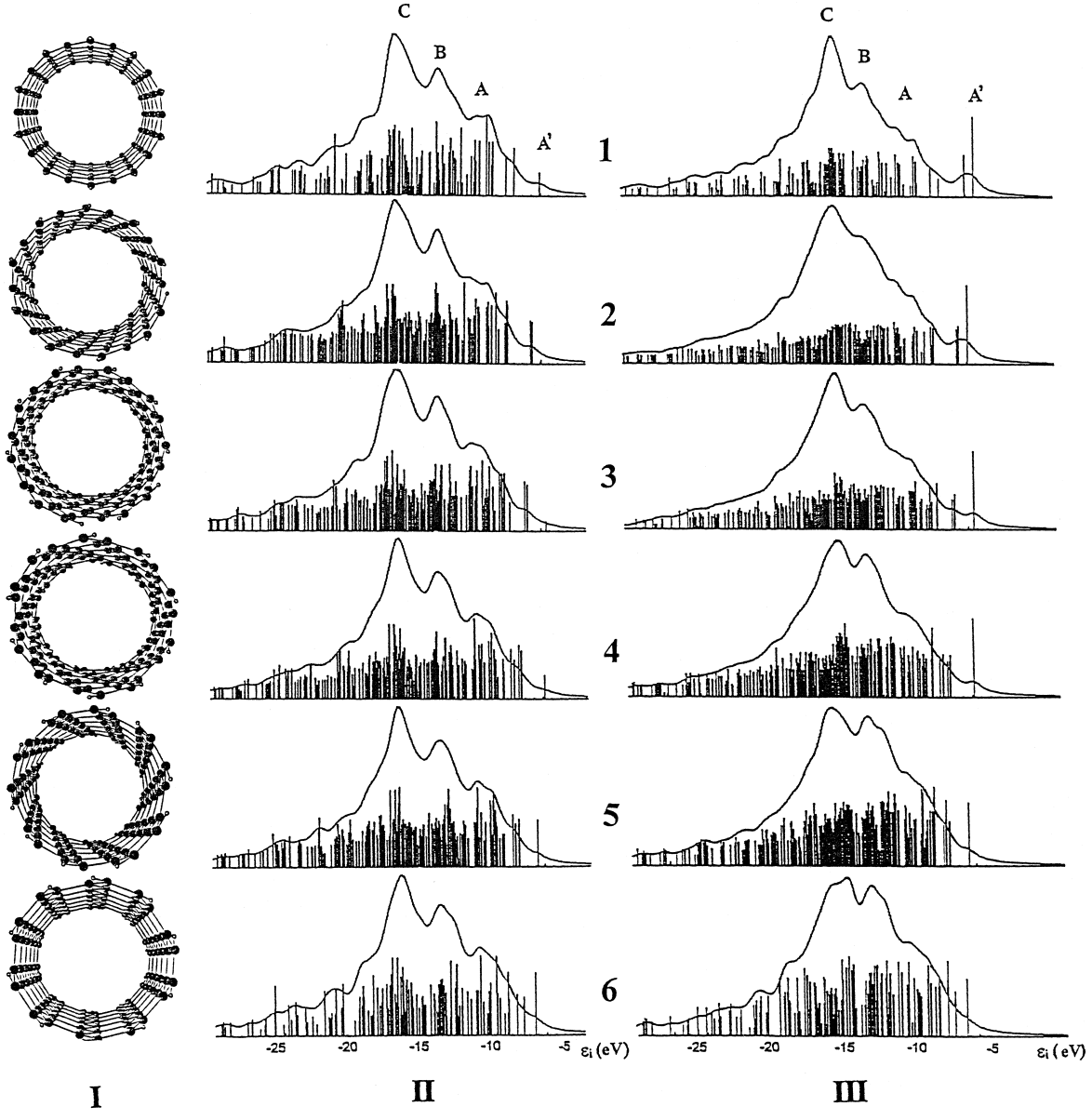

Fig. 3. (I) Perspective end-on view of (n,m) nanotube fragments considered in the calculations: (1) (10,0) zig-zag tube; (2) (9,1) tube; (3) (8,2) tube; (4) (7,3) tube; (5) (6,4) tube; (6) (5,5) armchair tube. Calculated X-ray spectra, based on the local densities of states at sites in the center (II) and at the exposed edge (III) of the tube fragments.

Carbon atoms at tube ends contribute significantly to the X-ray spectra of real samples containing short and defective tubes. To study the effect of tube ends on the X-ray spectra, we show the calculated CKα spectra of the 40 carbon atoms at the end of the tube fragments in Fig. 3(III). In contrast to the theoretical spectra of the tube centers, the spectra of the edge atoms change considerably across the nanotube series, from (10,0) to (5,5). The atoms at the open edge of the (10,0) zig-zag tube fragment are bound by strong σ bonds, which are reflected in the dominance of the peak C. The electrons at the open edge

of the (5,5) tube fragment, on the other hand, are shared evenly by the σ and π systems. The calculated spectra of edge atoms, shown in Fig. 3(III), primarily correspond to the electronic states near the open tube ends. Open-ended tubes are observed in the samples containing multiwall [32] as well as single-wall structures (Fig. 1.2). A small concentration of hydrogen (< 0.5 wt%), which is expected to be present in the soot during the arc-discharge evaporation of graphite, can lead to the formation of C–H bonds at the open tube ends [33].

The ends of most tubes are closed by hemispherical domes or polyhedra [2]. Scanning tunneling spectroscopy (STS) measurements show that the electronic structure of the valence band differs considerably between the body and the end of (n,0) tubes [34]. These data indicate an increase of the electronic density of states by localized states at the tube ends, and the appearance of an additional sharp maximum near the Fermi level. Then, also the intensity of peak A′ in the X-ray spectrum should increase accordingly, which is in agreement with our theoretical results for the (10,0) tube fragment. As seen by comparing Fig. 3(II) and Fig. 3(III), peak A′ appears more pronounced near the edge of the fragment, which may be either open or terminated by a cap than in the central part of the tube. The local electronic density of states near the tube ends has been found to depend significantly on tube diameter and chirality and only to a much lesser degree on the structure of the tube apex [35].

As seen in Fig. 2, the relative intensities of peaks A and B are enhanced with respect to the main peak C when comparing the X-ray spectrum of sample 2 with that of sample 1. The same intensity increase of peaks A and B is observed in the calculated spectra

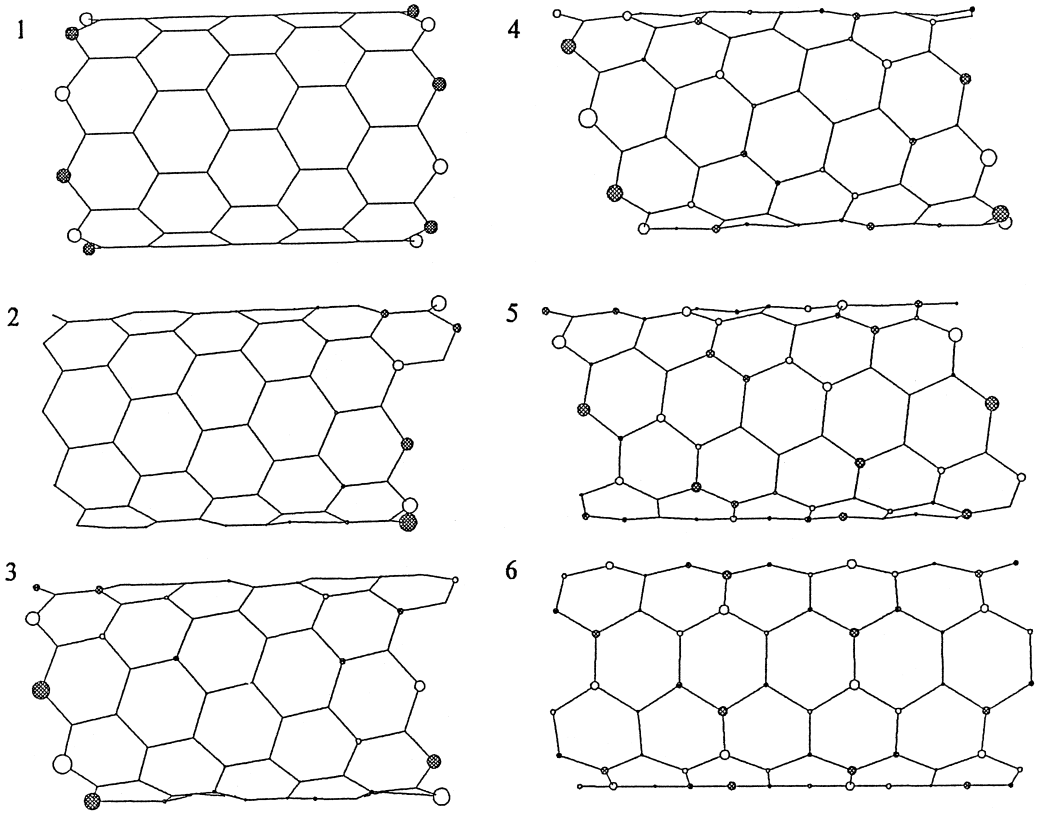

Fig. 4. Character of the HOMO in the (1) (10,0), (2) (9,1), (3) (8,2), (4) (7,3), (5) (6,4), and (6) the (5,5) tube. The circle radius at each site denotes the contribution of the corresponding atomic p-orbital to the HOMO, and the circle color denotes the phase.

of Fig. 3 when comparing armchair (m,m) to zig-zag $(n,0)$ tube fragments. This trend appears even more pronounced in the density of states of edge atoms, shown in Fig. 3(III) and should be best observable in X-ray spectra of short (m,m) nanotubes with a large fraction of edge atoms or defects. However, the local electronic densities of states at the edge and in the central part of $(n,0)$ zig-zag tubes are similar when comparing the relative intensities of peaks A, B and C. Consequently, a larger fraction of edge atoms or defects, occurring in short zig-zag-like tubes, is unlikely to change their X-ray spectra significantly. The only exception is a relative intensity increase of the low binding-energy peak A′ at the open end of zig-zag nanotubes. As seen in Fig. 2, this peak appears to be more pronounced in sample 1, taken from the cathode deposit, than in sample 2 obtained from the cold chamber walls, leading to the conclusion that short zig-zag nanotube fragments may be more abundant in the cathode deposit than at the chamber walls.

We have already mentioned that the shift of peak A′ towards lower binding energies, along with its intensity increase, is a characteristic of zig-zag-like tubes. It is also intriguing to study any other changes of the electronic structure, in particular that of the HOMO, as the nanotube geometry changes from a zig-zag-like to a more armchair like morphology. The character of the HOMO in the different nanotube fragments is shown in Fig. 4. The contribution of a radially oriented atomic p orbital at a particular site to the π-like HOMO is visualized by the radius of a circle at that site. The color of the circle denotes the phase of the particular p orbital (white circles denote an orbital directed 'radially in', black circles an orbital directed 'radially out'). We find the character of the HOMO changes drastically as the morphology transforms from zig-zag towards armchair-like. In nanotubes with a morphology close to that of zig-zag $(n,0)$ nanotubes, the HOMO (and also the LUMO) is predominantly localized at tube ends, where the dangling bonds may be saturated by hydrogen. In armchair-like nanotubes, on the other hand, atoms in the center and at the edge appear to participate evenly in the HOMO. Since the reactivity of nanotubes is closely related to the character of their frontier orbitals, we conclude that zig-zag nanotubes may be especially reactive near their growing edge. The relative inertness of armchair nanotubes, on the other hand, may be explained by the equally small participation of all tube sites in the HOMO.

5. Conclusions

Based on the present study, we believe that carbon soot, which is formed in the atmosphere of the arc-discharge apparatus, contains carbon nanotubes with structures that most closely resemble those of (m,m) 'armchair' nanotubes. Our calculations show that fragments of these tubes are the most thermodynamically stable. The difference between the X-ray spectra of samples produced under various synthetic conditions can be understood by comparing the theoretical spectra of zig-zag and armchair tubes. These differences are even more pronounced in systems with a large fraction of edge atoms, such as in short and defective tubes.

References

[1] W. Kratschmer, L.D. Lamb, K. Fostiropoulos, D.R. Huffman, Nature 347 (1990) 354.
[2] S. Iijima, Nature 354 (1991) 56.
[3] T.W. Ebbesen, P.M. Ajayan, Nature 358 (1992) 220.
[4] Y. Ando, S. Iijima, Jpn J. Appl. Phys. 32 (1993) L107.
[5] A.V. Okotrub, D.A. Romanov, A.L. Chuvilin, Yu.V.Shevtsov, A.K. Gutakovskii, L.G. Bulusheva, L.N. Mazalov, Phys. Low-Dim. Struct. 8/9 (1995) 139.
[6] S. Iijima, T. Ichihashi, Nature 363 (1993) 603.
[7] D.S. Bethune, C.H. Kiang, M.S. de Vries, G. Gorman, R. Savoy, J. Vazquez, R. Beyers, Nature 363 (1993) 605.
[8] X. Sun, C.-H. Kiang, M. Endo, K. Takeuchi, T. Furuta, M.S. Dresselhaus, Phys. Rev. B 54 (1996) R12629.
[9] M. Dresselhaus, G. Dresselhaus, P.C. Eklund, Science of Fullerene and Carbon Nanotubes (Academic Press, San Diego, CA, 1996).
[10] A. Thess, R. Lee, P. Nikolaev, H. Dai, P. Petit, J. Robert, C. Xu, Y.H. Lee, S.G. Kim, A.G. Rinzler, D.T. Colbert, G.E. Scuseria, D. Tomanek, J.E. Fischer, R.E. Smalley, Science 273 (1996) 483.
[11] L.-C. Qin, S. Iijima, H. Kataura, Y. Maniwa, S. Suzuki, Y. Achiba, Chem. Phys. Lett. 268 (1997) 101.
[12] J.M. Cowley, P. Nikolaev, A. Thess, R.E. Smalley, Chem. Phys. Lett. 265 (1997) 379.
[13] J.W. Mintmire, B.I. Dunlap, C.T. White, Phys. Rev. Lett. 68 (1992) 631.
[14] X. Blase, L.X. Benedict, E.L. Shirley, S.G. Louie, Phys. Rev. Lett. 72 (1994) 1978. 15.

[15] L. Chico, L.X. Benedict, S.G. Louie, M.L. Cohen, Phys. Rev. B 54 (1996) 2600.
[16] M.S. Dresselhaus, G. Dresselhaus, R. Saito, Solid State Commun. 84 (1992) 201.
[17] N. Hamada, S.-I. Sawada, A. Oshiyama, Phys. Rev. Lett. 68 (1992) 1579.
[18] E.Z. Kurmaev, S.A.N. Shaman, K.M. Kolobova, S.V. Shulepov, Carbon 24 (1986) 249.
[19] J. Kawai, K. Maeda, M. Takami, Y. Muramatsu, T. Hayashi, M. Motoyama, Y. Saito, J. Chem. Phys. 98 (1993) 3650.
[20] E.-K. Kortela, R. Manne, J. Phys. C: Solid State Phys. 7 (1974) 1749.
[21] D. Ostling, D. Tomanek, A. Rosen, Phys. Rev. B 55 (1997) 13980.
[22] A.V. Okotrub, Yu.V. Shevtsov, L.I. Nasonova, D.E. Sinyakov, O.A. Novosel'tsev, S.V. Trubin, V.S. Kravchenko, L.N. Mazalov, Instrum. Exp. Tech. 38 (1995) 131.
[23] A.V. Okotrub, A.L. Chuvilin, Yu.V. Shevtsov, A.K. Gutakovskii, L.I. Nasonova, L.N. Mazalov, Recent Adv. Chem. Phys. Fullerenes Relat. Mater. 2 (1995) 678.
[24] A.V. Okotrub, V.D. Yumatov, L.N. Mazalov, G.S. Belikova, T.M. Okhrimenko, Zh. Strukt. Khim. 29 (1988) 167.
[25] J.J.P. Stewart, J. Comp. Chem. 10 (1989) 209.
[26] M.W. Schmidt, K.K. Baldridge, J.A. Boatz, S.T. Elbert, M.S. Gordon, J.H. Jensen, S. Kosoki, N. Matsunaga, K.A. Nguyen, S.J. Su, T.L. Windus, M. Dupluis, J.A. Montgomery, J. Comput. Chem. 14 (1993) 1347.
[27] R. Saito, M. Fujita, G. Dresselhaus, M.S. Dresselhaus, Appl. Phys. Lett. 60 (1992) 2204.
[28] L.G. Bulusheva, A.V. Okotrub, D.A. Romanov, D. Tomanek, J. Phys. Chem. A (1998).
[29] M.R. Pederson, J.Q. Broughton, Phys. Rev. Lett. 69 (1992) 2689.
[30] Y.H. Lee, S.G. Kim, D. Tomanek, Phys. Rev. Lett. 78 (1997) 2393.
[31] L.N. Mazalov, V.D. Yumatov, V.V. Murakhtanov, F.H. Gel'mukhanov, G.N. Dolenko, A.V. Kondratenko, X-Ray Spectra of Molecules (Novosibirsk, Nauka, 1977).
[32] S. Iijima, P.M. Ajayan, T. Ichihashi, Phys. Rev. Lett. 69 (1992) 3100.
[33] A.V. Okotrub, Yu.V. Shevtsov, L.I. Nasonova, D.E. Sinyakov, A.L. Chuvilin, A.K. Gutakovskii, L.N. Mazalov, Neorgan. Mater. 32 (1996) 858.
[34] D.L. Carroll, P. Redlich, P.M. Ajayan, J.C. Charlier, X. Blase, A. De Vita, R. Car, Phys. Rev. Lett. 78 (1997) 2811.
[35] R. Tamura, M. Tsukada, Phys. Rev. B 52 (1995) 6015.